



Structure-based *de novo* design of Eya2 phosphatase inhibitors

Hwangseo Park^{a,*}, Seong Eon Ryu^b, Seung Jun Kim^{c,**}

^a Department of Bioscience and Biotechnology, Sejong University, 98 Kunja-Dong, Kwangjin-Ku, Seoul 143-747, Republic of Korea

^b Department of Bio Engineering, Hanyang University, Seongdong-Gu, Seoul 133-791, Republic of Korea

^c Medical Proteomics Research Center, Korea Research Institute of Bioscience and Biotechnology, 52 Eoeun-Dong, Yuseong-Gu, Daejeon 305-600, Republic of Korea

ARTICLE INFO

Article history:

Accepted 27 May 2012

Available online 5 June 2012

Keywords:

De novo design
Eya2 phosphatase
Inhibitor
Chelating group
Anticancer agents

ABSTRACT

Although Eyes absent protein tyrosine phosphatases proved to be involved in various human cancers by a series of persuasive experimental evidence, only a very few number of small-molecule inhibitors have been reported so far. We have been able to identify 29 novel inhibitors of Eyes absent homologue 2 (Eya2) by means of a structure-based *de novo* design with the two known inhibitor scaffolds that contain a proper chelating group for the active-site Mg^{2+} ion. Because these newly found inhibitors were screened for having desirable physicochemical properties as a drug candidate and exhibited a moderate inhibitory activity with IC_{50} values ranging from 6 to 50 μM , they deserve consideration for further investigation to develop new anticancer medicines. Structural features relevant to the stabilization of the identified inhibitors in the active site of Eya2 phosphatase are discussed in detail.

© 2012 Elsevier Inc. All rights reserved.

1. Introduction

Protein tyrosine phosphatases (PTPs) hydrolyze the phosphorylated tyrosine residue on various protein substrates and thereby serve as a hallmark in the cellular signal transductions. It is characteristic of Eyes absent PTPs (Eyas) to use the side-chain aspartyl group and a metal ion as the nucleophile and the Lewis acid catalyst in the hydrolysis reactions, respectively, instead of the cysteine and arginine residues employed by most of the other PTPs [1,2]. Eyas may be involved in a variety of cancers because they play a crucial role in determining the life and death fate in response to genotoxic stress. For example, Eyes absent homologue 2 (Eya2) proved to be up-regulated in ovarian cancer [3] and lung adenocarcinoma [4]. The inhibition of Eya4 reduced the tumorigenic properties of the malignant peripheral nerve sheath tumor *in vitro* and resulted in cell death *in vivo* [5]. Furthermore, the tyrosine phosphatase activity of Eya was shown to be responsible for the migration, invasion, and transformation of tumor cells [6]. The inhibition of the catalytic activity of Eyas can thus be a promising strategy for the development of therapeutics for cancers.

In recent years, the X-ray crystal structures of Eya2 were reported both in the resting and in the ligand-bound forms [7,8]. The presence of structural information about the nature of the interactions between Eya2 phosphatase and its small-molecule inhibitor can make it a plausible task to design a good lead

compound for anticancer drugs. Nonetheless, the discovery of Eya inhibitors has lagged behind the pharmacological and structural studies. To the best of our knowledge, only a very few number of small-molecule Eya inhibitors have been reported so far including beryllium trifluoride (BeF_3). In the previous work, we reported the first example for the discovery of novel classes of Eya2 phosphatase inhibitors by means of the structure-based virtual screening with docking simulations and *in vitro* enzyme assay [9]. The potent inhibitors found in this study included the two scaffolds, **1** (2-amino-3-(3-methyl-4-oxo-2-thioxo-thiazolidin-5-ylidenemethyl)-pyrido[1,2-*a*]pyrimidin-4-one) and **2** (5-(3,4-dihydroxy-benzylidene)-2-phenylamino-thiazol-4-one) as shown in Fig. 1.

Using the structure-based *de novo* design method, we aim in the present study to find the derivatives of the two inhibitor scaffolds that have both a high inhibitory activity against Eya2 phosphatase and good physicochemical properties as a drug candidate. The characteristic feature that discriminates our *de novo* design approach from the others lies in the implementation of an accurate solvation model in calculating the binding free energy between Eya2 phosphatase and the putative inhibitors, which would have an effect of enhancing the accuracy in predicting the binding affinity [10]. On the basis of the results for docking simulations, we will also address the binding forces that are responsible for stabilization of the newly identified inhibitors in the active site of Eya2 phosphatase.

2. Methods

LigBuilder program [11] was used in the structure-based *de novo* design of Eya2 phosphatase inhibitors using its X-ray

* Corresponding author. Tel.: +82 2 3408 3766; fax: +82 2 3408 4334.

** Corresponding author. Tel.: +82 42 860 4242; fax: +82 42 860 4598.

E-mail addresses: hspark@sejong.ac.kr (H. Park), ksj@kribb.re.kr (S.J. Kim).

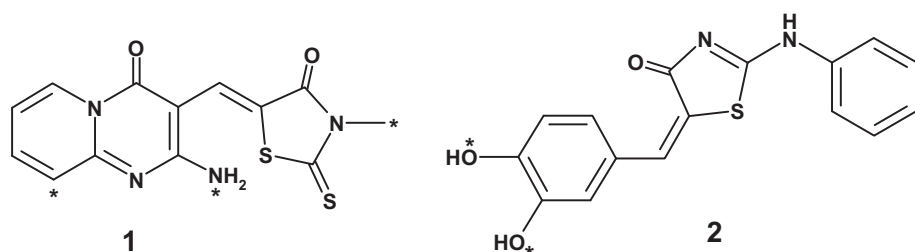


Fig. 1. Chemical structures of the two inhibitor scaffolds under investigation. Each asterisk indicates the position of substitution.

crystal structure in complex with the substrate-analog inhibitor BeF_3 (PDB ID: 3HB0) [7]. In order to score various derivatives of a given inhibitor scaffold according to the relative binding affinity for the target protein, the program usually employs the empirical binding free energy function including van der Waals, hydrogen bond, electrostatic, and entropic terms [12]. Gasteiger–Marsili atomic charges [13] were used for both proteins and ligands in the calculation of the electrostatic interaction term. The current scoring function of LigBuilder lacks a solvation term although the effects of ligand solvation have been shown to be critically important in protein–ligand association [10]. Therefore, the solvation free energy function developed by Kang et al. [14] was added to the original scoring function of LigBuilder to improve the accuracy in predicting the relative potencies of the derivatives. The two inhibitor scaffolds identified in the previous study (**1** and **2** in Fig. 1) were used as the starting structures of *de novo* design. The first step to design the new derivatives was to analyze the binding pocket in the active site using the POCKET module. The structures of Eya2 phosphatase in complex with **1** and **2** obtained from docking simulations with the AutoDock program [15] were used as the input for the POCKET module to find the key interaction residues in the active site. The next step involved the generation of the derivatives of the two inhibitor scaffolds by applying the genetic algorithm as implemented in the GROW module. The bioavailability rules were also applied to screen the derivatives with good physicochemical properties as a drug candidate [16].

In this structure-based *de novo* design, we explored the substituent space on the two promising cores at four or five positions to identify the substituents that were expected to have the enhanced inhibitory activity against Eya2 phosphatase. This could be possible by computing the binding free energies for varying substituents at the substitution positions with the core structure being kept fixed. Structures were thus evolved from the hydrogens attached to the substitution points of the molecular cores. For each of the two inhibitor scaffolds, approximately 100,000 derivatives were generated and scored according to the calculated binding affinities. The 500 top-scored molecules for each scaffold were then checked for commercial availability. Actually, the derivatives of **1** and **2** were scored according to the binding free energy associated with the formation of protein–ligand complex in aqueous solution (ΔG_b^{aq}) that was given by the difference between that in the gas phase (ΔG_b^{gas}) and solvation free energy of the ligand of interest (ΔG^{sol}) [17]. We compared the two energy components to estimate their relative contributions to ΔG_b^{aq} . ΔG_b^{gas} and ΔG^{sol} values were found to range from -25.1 to -17.6 kcal/mol, and from -18.7 to -6.2 kcal/mol, respectively, for the 500 hit compounds designed from scaffold **1**. In case of the top-scored derivatives of scaffold **2**, the minimum and maximum energy values amount to -24.0 and -16.9 kcal/mol for ΔG_b^{gas} , respectively, as compared to -19.2 and -6.1 kcal/mol for ΔG^{sol} . Although the absolute values of ΔG^{sol} appear to be smaller than those of ΔG_b^{gas} , the

wider range of ΔG^{sol} indicates that it may serve as a determinant for the binding affinities of structurally similar inhibitors of Eya2 phosphatase.

Finally, 73 and 41 commercially available derivatives of **1** and **2** were respectively purchased from compound suppliers and tested for inhibitory activities against Eya2 phosphatase. Enzyme assays were performed using 6,8-difluoro-4-methylumbelliferyl phosphate (DIFMUP) as a substrate at 25°C and pH 6.5 in the presence or absence of an inhibitor in the reaction vessel including 20 mM MES, 150 mM NaCl, 5 mM DTT, and 2 mM MgCl_2 . After adding purified Eya2 (50 nM) and DIFMUP (20 μM), the reactions were allowed to proceed for 90 min at room temperature, and were stopped by adding sodium orthovanadate (1 mM). The fluorescence intensity was measured (355 nm excitation and 460 nm emission) using a plate reader. IC_{50} values were determined directly from the regression curves constructed using the tested inhibitors. This procedure was repeated in duplicate for all of the putative inhibitors to obtain their average IC_{50} values. BeF_3 was used as a reference inhibitor, whose IC_{50} value was measured to be 54.4 μM in this experiment. Inhibition by BeF_3 was performed by reacting Eya2 with varying concentration of BeCl_2 and NaF (100-fold excess) for 1 h.

3. Results and discussion

As a result of the enzyme assays, seventeen and twelve derivatives of **1** and **2** were respectively found to inhibit the catalytic activity of Eya2 phosphatase by more than 50% at the concentration of 50 μM . Table 1 lists the structures and inhibitory activities of the newly identified inhibitors derived from **1**. We note that most of the derivatives with inhibitory activity prefer the hydrogen atom or the small substituents at R1, R2, and R4 positions, which is not surprising for the flat and shallow active site of Eya2 [7]. On the other hand, the derivatives with relatively bulky groups such as aromatic rings and long alkyl chains at R3 and R5 positions are also found to exhibit a high inhibitory activity. For example, a potent inhibitor (**1o**) with micromolar activity can be obtained with the substitutions of butanol and anisole moieties at R3 and R5 positions, respectively. The most potent inhibitor (**1g**) can be generated when the methyl group is substituted at R1 and R3, and the phenyl group at R5 position. It is noteworthy that the potent Eya2 phosphatase inhibitors with micromolar activity can also be obtained with the substitution of benzo[1,3]dioxole moiety at R5 position (**1h**, **1i**, and **1m**). Because all of the inhibitors shown in Table 1 reveal a high inhibitory activity with IC_{50} values lower than 22 μM and were screened for having the desirable physicochemical properties as a drug candidate, they deserve consideration for further investigation to develop anticancer medicines.

It should be noted that each substituent in Table 1 involves the substitutions on the terminal amine group attached to pyrido[1,2-*a*]pyrimidin-4-one ring although the substitution may have an effect of lowering the binding affinity due to the weakening of hydrogen bond interactions with the negatively charged Asp/Glu

Table 1
Structures and inhibitory activities of the derivatives of **1**.

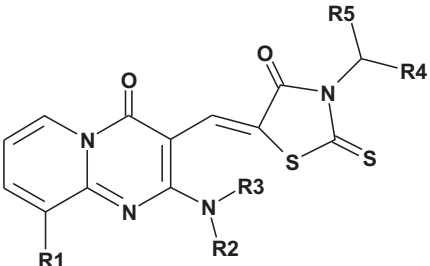
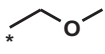
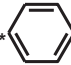
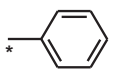
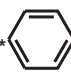
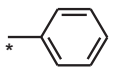
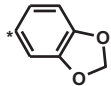
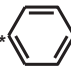
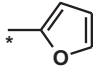
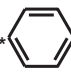
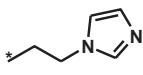
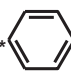
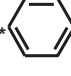
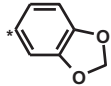
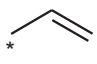
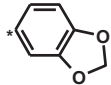
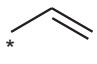
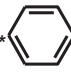
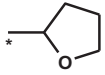
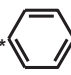
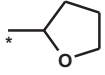
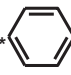
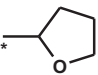
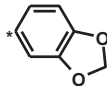

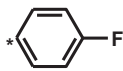

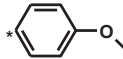


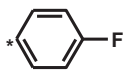


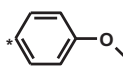
						
	R1	R2 ^a	R3 ^a	R4	R5 ^a	IC ₅₀
1	H	H	H	H	H	60.2
1a	H	H		H		20.6
1b	CH ₃	CH ₃		H		20.5
1c	H	CH ₃		H		21.3
1d	H	H	CH ₂ CH ₃	H		11.8
1e	CH ₃	H		H		13.8
1f	CH ₃	H		H		7.9
1g	CH ₃	H	CH ₃	H		6.6
1h	H	H	CH ₂ CH ₃	H		7.3
1i	CH ₃	H		H		7.4
1j	CH ₃	H		CH ₃		14.3
1k	H	H		H		8.6
1l	H	H		CH ₃		7.7

Table 1 (Continued)

	R1	R2 ^a	R3 ^a	R4	R5 ^a	IC ₅₀
1m	H	H		H		8.4
1n	CH ₃	H		H		10.5
1o	CH ₃	H		H		8.6
1p	H			H		12.1
1q	H			H		14.4

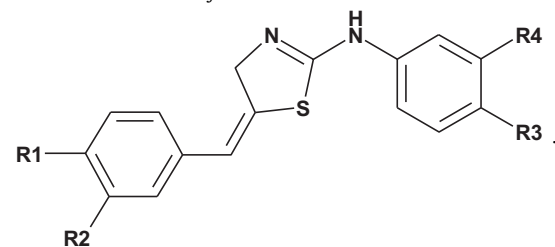
^a Asterisk indicates the atom attached to the position of substitution.


residues in the active site. Indeed, ΔG_b^{gas} values are found to increase from -23.5 to -22.8 kcal/mol with the substitution of a methyl group on the terminal amine group. However, the same substitution may enhance the binding of the inhibitor in the active site by reducing the desolvation cost for enzyme–inhibitor complexation. We note in this regard that the solvation free energy also increases from -12.8 to -10.1 kcal/mol due to the substitution of a methyl group. Therefore, the substitution seems to have a positive effect on the binding affinity by reducing the desolvation cost for complexation to a greater extent than the weakening of enzyme–inhibitor interactions.

Twelve derivatives of **2** were found to have inhibitory activity against Eya2 phosphatase with IC₅₀ values ranging from 10 to 50 μM , whose structures and inhibitory activities are summarized

in Table 2. We see that the most potent derivative (**2e**) possesses the $-\text{OH}$ moiety at R1 and R2 positions. The change of either hydroxy group to methoxy or ethoxy group leads to a decrease in the inhibitory activity irrespective of the substitution at the other positions. The two $-\text{OH}$ groups seem to interact with the active-site Mg^{2+} ion, the deactivation of which is necessary for the effective inhibition of Eya2 phosphatase. It is a similar structural feature to the inhibitorily active derivatives of **1** that small substituents are preferred to large ones at most of the substitutions positions. Because most of the substituents in Table 2 but the methyl group are polar, hydrogen bond and dipole–dipole interactions seem to be more significant than hydrophobic interactions for the inhibitors to be stabilized in the active site of Eya2.

Table 2
Structures and inhibitory activities of the derivatives of **2**.



	R1 ^a	R2 ^a	R3	R4	IC ₅₀
2	OH	OH	H	H	12.3
2a	OH	OCH ₃	H	F	21.9
2b			H	F	31.1
2c	OCH ₃	OH	H	Cl	47.5
2d	OH	OCH ₃	CH ₃	CH ₃	42.0
2e	OH	OH	CH ₃	CH ₃	10.7
2f	OCH ₂ CH ₃	OH	H	H	44.4
2g	OCH ₂ CH ₃	OH	CH ₃	H	42.6
2h	OCH ₂ CH ₃	OH	OH	H	26.5
2i	OCH ₃	OH	H	H	29.9
2j	OH	OCH ₃	H	OH	18.5
2k	OCH ₂ CH ₃	OH	Cl	Cl	25.7
2l	OH	OCH ₃	CH ₃	H	17.7

^a Asterisk indicates the atom attached to the position of substitution.

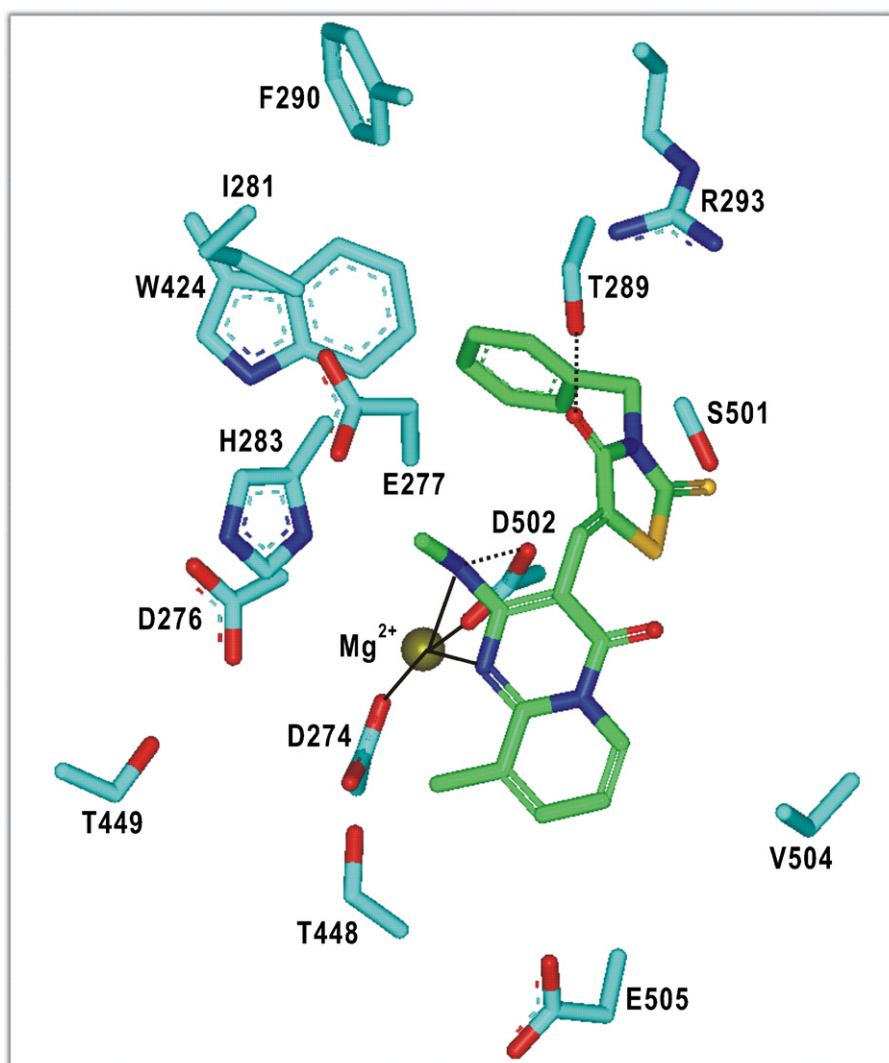


Fig. 2. Calculated binding mode of **1g** in the active site of Eya2 phosphatase. Carbon atoms of the protein and the ligand are indicated in cyan and green, respectively. Solid and dotted lines indicate the coordination to the central Mg^{2+} ion and the hydrogen bond, respectively.

In the *de novo* design of scaffold **2**, it seems to be impossible to identify better derivatives than the benzene-1,2-diol group in itself. For example, we find that the substitution of a methoxy for a hydroxyl moiety on the terminal phenyl ring raise the ΔG_b^{gas} value from -24.8 to -21.2 kcal/mol due to the disappearance of strong hydrogen-bond interactions of the phenolic group with the active site residues of Eya2 phosphatase. Although the same substitution is found to reduce the desolvation cost for complexation by 2.9 kcal/mol, this is apparently insufficient to compensate for 3.6 kcal/mol loss of the interaction energy (ΔG_b^{gas}) in the enzyme–inhibitor complex. Consistent with these energetic features, the derivatives with the benzene-1,2-diol group are most abundant in the virtual hits derived from *de novo* design. However, most of them are found to be commercially unavailable at present, which prevents us from identifying the new potent Eya2 phosphatase inhibitors. Related with the substitution effects on binding affinity, it is noteworthy that the similar methyl substitution causes the more loss of stabilization energy in scaffold **2** than **1**. This is actually not surprising because the phenol moiety can form the stronger hydrogen bonds with the negatively charged groups than the amine moiety due to the higher acidity of the former than the latter.

To obtain some structural insight into the inhibitory mechanisms by the newly identified Eya2 phosphatase inhibitors, their

binding modes in the active site were investigated using the AutoDock program [15]. The calculated binding mode of the most potent inhibitor (**1g**) among the derivatives of **1** is shown in Fig. 2. In this calculated Eya2–**1g** complex, 2-aminopyrido[1,2-*a*]pyrimidin-4-one group of **1g** is accommodated in a small binding pocket comprising the side chains of Asp274, Thr448, Val504, and Glu505 at the bottom of the active site. The two nitrogen atoms in the 2-aminopyrido[1,2-*a*]pyrimidin-4-one moiety are coordinated to the Mg^{2+} ion in the active site with the associated N...Mg distances of 2.4–2.5 Å. This confirms that the deactivation of the active-site Mg^{2+} ion by a proper chelating group should be necessary for the inhibition of Eya2 phosphatase. The methylamine group of **1g** coordinated to the Mg^{2+} ion appears to donate a hydrogen bond to the side-chain carboxylate ion of Asp502 that also serve as a ligand for the Mg^{2+} ion. Therefore, this hydrogen bond seems to play a significant role in maintaining the coordination of the 2-aminopyrido[1,2-*a*]pyrimidin-4-one moiety to the Mg^{2+} ion as well as in increasing the binding affinity of **1g** in the active site.

Related with the preference for small substituents at R2 position (Table 1), it should be noted that the methylamine group coordinated to the Mg^{2+} ion resides in close proximity to the side chains of Asp276, Glu277, His283, and Asp502. This indicates that the substitution of a bulky group at R2 position would lower the

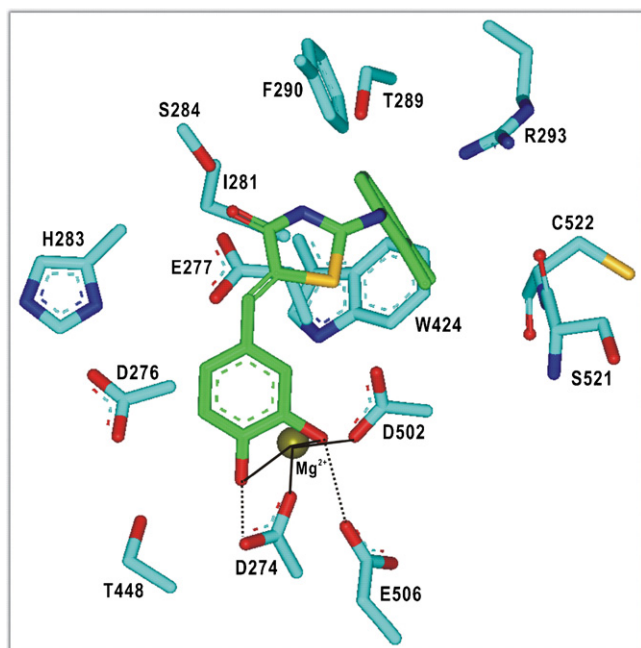


Fig. 3. Calculated binding mode of **2e** in the active site of Eya2 phosphatase. Solid and dotted lines indicate the coordination to the central Mg^{2+} ion and the hydrogen bond, respectively.

inhibitory activity due to the resulting repulsive interactions with those active-site residues. An affinity-enhancing hydrogen bond is also established between the carbonyl oxygen of **1g** and the side-chain hydroxy group of Thr289 at the top of the active site. The inhibitor **1g** can be further stabilized in the active site by establishing the hydrophobic interactions between its nonpolar groups and the side chains of Ile281, His283, Phe290, Trp424, and Val504. It is also worth noting that the terminal benzylic position of **1g** stays close to the side chains of Thr289, Arg293, and Ser501, which can be invoked to explain that only small substituents may be favored at R4 position to retain the inhibitory activity (Table 1). On the basis of the structural features derived from docking simulations, it can be argued that **1g** should be capable of impairing the enzymatic activity of Eya2 by binding in the active site through the simultaneous establishment of the multiple hydrogen bonds and hydrophobic interactions in addition to the chelation of the Mg^{2+} ion.

Fig. 3 shows the lowest-energy binding mode of **2e** in the active site of Eya2. In this calculated complex, the role of chelator for the Mg^{2+} ion appears to be played by the two terminal hydroxy moieties with similar coordination distances to those in the Eya2-**1g** complex. However, the metal–ligand interactions in the Eya2-**2e** complex seem to be weaker than those in the Eya2-**1g** complex due to the lower basicity of oxygen than nitrogen ligands. We note that both hydroxy ligands for the Mg^{2+} ion donate a hydrogen bond to the side-chain carboxylate ions of Asp274 and Glu506. These two hydrogen bonds are most likely to play a role of positioning the coordination of the two hydroxy groups to the Mg^{2+} ion because both are established in the vicinity of the Mg^{2+} ion cluster at the bottom of the active site. These two hydrogen bonds would also have an effect of facilitating the coordination of the two hydroxy groups to the Mg^{2+} ion through the partial deprotonation by the negatively charged side chains. The important roles of the hydrogen bonds involving the two hydroxy moieties in binding at the active site can be invoked to explain the higher inhibitory activity of **2e** than the other derivatives of **2** with methoxy or ethoxy groups at one of the R1 and R2 positions (Table 2), which would be able to donate only one hydrogen bond to the side-chain carboxylate groups.

As in the Eya2-**1g** complex, **2e** forms van der Waals contacts with the side chains of Ile281, His283, Phe290, and Trp424, which should also be a significant binding force stabilizing the inhibitor in the active site of Eya2. The terminal *o*-xylene group of **2e** seems to be optimally accommodated in the binding pocket at the top of the active site comprising Thr289, Phe290, Arg293, Trp424, Ser521, and Cys522 because all of the associated interatomic distances fall within 5 Å. Such a small size the binding pocket can be the reason for the preference of small substituents at R3 and R4 positions (Table 2). Because the number of hydrogen bonds is the same and the hydrophobic interactions are established in a similar fashion in Eya2-**1g** and Eya2-**2e** complexes, a little lower inhibitory activity of **2e** than **1g** can be attributed to the weaker coordination of the former to the active-site Mg^{2+} ion than the latter.

Despite the improvement of the scoring function by implementing of the ligand solvation effects, it seems to need further modifications because potent Eya2 phosphatase inhibitors with submicromolar activity are not discovered in this study. Of the various energy terms, the most significant contribution to the scoring function can be made by the entropy term [15], which is a measure of the unfavorable entropy of ligand binding due to the restriction of conformational degrees of freedom. Despite such an importance, the entropic term has been roughly approximated as a simple linear function with respect to the number of sp^3 bonds due to the difficulty in the precise description for the entropy change in protein–ligand association. Thus, the development of a proper entropic term seems to be necessary to further improve the efficiency of *de novo* design and virtual screening.

4. Conclusions

In this study, we have identified 29 inhibitors of Eya2 phosphatase by applying structure-based *de novo* design using the two existing inhibitor scaffolds. These inhibitors revealed moderate inhibitory activities with IC_{50} values ranging from 6 to 50 μM , and were screened for having desirable physicochemical properties as a drug candidate. Therefore, each of them deserves consideration for further investigation to develop new anticancer medicines. Detailed binding mode analyses with docking simulations show that besides the chelation of the Mg^{2+} ion, the inhibitors can be stabilized in the active site through the simultaneous establishment of the multiple hydrogen bonds with polar residues and the van der Waals contacts with hydrophobic residues.

Acknowledgments

This work was supported by a grant (No. 2011-0030027) from the National Research Foundation of Korea Government funded by the Ministry of Education, Science, and Technology.

References

- [1] J.P. Rayapureddi, C. Kattamuri, B.D. Steinmetz, B.J. Frankfort, E.J. Ostrin, G. Mardon, R.S. Hegde, Eyes absent represents a class of protein tyrosine phosphatases, *Nature* 426 (2003) 295–298.
- [2] A. Alonso, J. Sasin, N. Bottini, I. Friedberg, I. Friedberg, A. Osterman, A. Godzik, T. Hunter, J. Dixon, T. Mustelin, Protein tyrosine phosphatases in the human genome, *Cell* 117 (2004) 699–711.
- [3] L. Zhang, N. Yang, J. Huang, R.J. Buckanovich, S. Liang, A. Barchetti, C. Vezzani, A. O'Brien-Jenkins, J. Wang, M.R. Ward, M.C. Courreges, S. Fracchioli, A. Medina, D. Katsaros, B.L. Weber, G. Coukos, Transcriptional coactivator *Drosophila* eyes absent homologue 2 is up-regulated in epithelial ovarian cancer and promotes tumor growth, *Cancer Research* 65 (2005) 925–932.
- [4] J. Guo, C. Liang, L. Ding, N. Zhou, Q. Ye, *Drosophila* eyes absent homologue 2 is up-regulated in lung adenocarcinoma, *Chinese-German Journal of Clinical Oncology* 8 (2009) 681–684.
- [5] S.J. Miller, Z.D. Lan, A. Hardiman, J. Wu, J.J. Kordich, D.M. Patmore, R.S. Hegde, T.P. Cripe, J.A. Cancelas, M.H. Collins, N. Ratner, Inhibition of eyes absent homolog 4 expression induces malignant peripheral nerve sheath tumor necrosis, *Oncogene* 29 (2010) 368–379.

- [6] R.N. Pandey, R. Rani, E.-J. Yeo, M. Spencer, S. Hu, R.A. Lang, R.S. Hegde, The eyes absent phosphatase-transactivator proteins promote proliferation, transformation, migration, and invasion of tumor cells, *Oncogene* 29 (2010) 3715–3722.
- [7] S.-K. Jung, D.G. Jeong, S.J. Chung, J.H. Kim, B.C. Park, N.K. Tonks, S.E. Ryu, S.J. Kim, Crystal structure of ED-Eya2: insight into dual roles as a protein tyrosine phosphatase and a transcription factor, *FASEB Journal* 24 (2010) 560–569.
- [8] N. Krishnan, D.G. Jeong, S.-K. Jung, S.E. Ryu, A. Xiao, C.D. Allis, S.J. Kim, N.K. Tonks, Dephosphorylation of the C-terminal tyrosyl residue of the DNA damage-related histone H2A.X is mediated by the protein phosphatase eyes absent, *Journal of Biological Chemistry* 284 (2009) 16066–16070.
- [9] H. Park, S.-K. Jung, K.R. Yu, J.H. Kim, Y.-S. Kim, J.H. Ko, B.C. Park, S.J. Kim, Structure-based virtual screening approach to the discovery of novel inhibitors of eyes absent 2 phosphatase with various metal chelating moieties, *Chemical Biology and Drug Design* 78 (2011) 642–650.
- [10] H. Park, J.-Y. Jeon, S.Y. Kim, D.G. Jeong, S.E. Ryu, Identification of novel inhibitors of mitogen-activated protein kinase phosphatase-1 with structure-based virtual screening, *Journal of Computer-Aided Molecular Design* 25 (2011) 469–475.
- [11] R. Wang, Y. Gao, L. Lai, LigBuilder., A multi-purpose program for structure-based drug design, *Journal of Molecular Modeling* 6 (2000) 498–516.
- [12] R. Wang, L. Liu, L. Lai, Y. Tang, SCORE: a new empirical method for estimating the binding affinity of a protein–ligand complex, *Journal of Molecular Modeling* 4 (1998) 379–394.
- [13] J. Gasteiger, M. Marsili, Iterative partial equalization of orbital electronegativity – a rapid access to atomic charges, *Tetrahedron* 36 (1980) 3219–3228.
- [14] H. Kang, H. Choi, H. Park, Prediction of molecular solvation free energy based on the optimization of atomic solvation parameters with genetic algorithm, *Journal of Chemical Information and Modeling* 47 (2007) 509–514.
- [15] G.M. Morris, D.S. Goodsell, R.S. Halliday, R. Huey, W.E. Hart, R.K. Belew, A.J. Olson, Automated docking using a Lamarckian genetic algorithm and an empirical binding free energy function, *Journal of Computational Chemistry* 19 (1998) 1639–1662.
- [16] C.A. Lipinski, F. Lombardo, B.W. Dominy, P.J. Feeney, Experimental, computational approaches to estimate solubility and permeability in drug discovery and development settings, *Advanced Drug Delivery Reviews* 23 (1997) 3–20.
- [17] B.K. Shoichet, A.R. Leach, I.D. Kuntz, Ligand solvation in molecular docking, *Proteins* 34 (1999) 4–16.